Fast Adaptive Equalizers for Narrow-Band TDMA Mobile Radio

Giovanna D'Aria, Roberto Piermarini, *Member, IEEE*, and Valerio Zingarelli, *Member, IEEE*

Abstract—**The future European cellular digital mobile radio system in the 900-MHz band adopts a narrow-band time division multiple access (TDMA) with GMSK modulation and a burst-type transmission based on a basic time slot consisting of a very short preamble (26-bit long) for synchronization and equalizer training purposes and of an information data section of 116 bits. Consequently, very fast adaptation methods are necessary to cope with the time- and frequency-selective distortions produced by Rayleigh and multipath fadings. This paper introduces a few theoretical aspects for the application of recursive least squares (RLS) adaptation algorithms to the narrow-band TDMA mobile radio system and gives the relevant performance results for the fast Kalman algorithm, which turns out to be suitable for the considered application. In particular, signature curves, bit error rate, speed of convergence, steady-state behavior, numerical stability, required accuracy, and hardware complexity are discussed. Both linear transversal and nonlinear decision-feedback equalizers are considered.**

I. Introduction

THE continuing growth of mobile telephone traffic and the requirement of integration with the digital communications facilities have spurred the research and development of a new high-capacity pan-European digital mobile radio system to put into service in the 1990's [1]. This system adopts time division multiple access (TDMA), with eight channels per carrier. The structure of each signal burst (or basic time slot) is depicted in Fig. 1, as stated by the recommendation [2] of the ETSI/GSM (European Telecommunications Standards Institute/Groupe Spécial Mobiles).

The modulating data signal rate is 270.8 kb/s; the information bits are split into two groups of 58 b by a preamble sequence, 26-b long, that enables synchronization and adaptive equalizer training (or channel estimation). Different preambles are used to discriminate cochannel interference. The selection of proper preamble sequences is a very important topic, as discussed in what follows. The operation of the receiver assumes the storage of the received time slot and then its processing.

Adaptive baseband equalization is necessary in the GSM mobile radio system because the transmission rate is greater than the "coherence bandwidth" [3]. In this case the frequency-selective distortions due to multipath propagation produce intersymbol interference, which is one of the dominant disturbance factors in narrow-band TDMA systems, together with the time-dispersive Rayleigh fading.

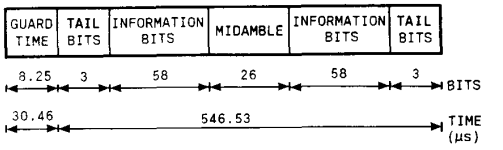

Fig. 1. Basic time slot structure.

Two main classes of adaptive receivers can be considered. The first class encompasses adaptive equalizers such as the linear transversal, the nonlinear decision-feedback, and the lattice equalizers [4]. The second class includes receivers employing maximum likelihood sequence estimation (MLSE), e.g., the Viterbi algorithm, [4], [5], made adaptive at least during the preamble period by means of some sort of channel estimation. The computational and storage requirements of the MLSE receiver increase exponentially with the duration of the channel impulse response. Moreover, the receiver complexity is further increased by the presence of adaptive prefiltering [5], required at high vehicle speeds, when the tracking of rapidly time-varying distortions is needed. On the other hand, with the time slot structure described above, the MLSE receiver compares favorably with the adaptive equalizers of the first class from the complexity point of view when the number of significant intersymbol interference components are limited to 4 and the propagation characteristics are stationary during the active part of the bursts (i.e., for vehicle speeds lower than about 100 km/h).

These considerations lead to the study and development of equalizers of the first class with very fast convergence properties during short preamble training sequences and fast tracking properties during the information data transmission, which are fundamental when the amplitude characteristics of the channel transfer function can vary at a rate of 100 dB/s and 30 MHz/s, [13].

This paper also shows that the simple and commonly used stochastic gradient-type algorithms are not suitable to our purpose. On the contrary, the adaptation algorithms derived from the least squares (LS) cost functions [4] have in general fast convergence and tracking capabilities. In particular, the Kalman-type algorithms [4], [7], [8] appear to be the fastest ones of this class. On the other hand, these Kalman-type algorithms are rather complex and need some assumption on the statistics of the equalizer's output error and on the

Manuscript received August 15, 1989; revised October 9, 1989 and March 27, 1990.

G. D'Aria is with CSELT (Centro Studi e Laboratori Telecomunicazioni), I 10148 Torino, Italy.

R. Piermarini is with SSGRR (Scuola Superiore Guglielmo Reiss Romoli), I 67010 L'Aquila, Italy.

V. Zingarelli was with CSELT, Torino, Italy. He is now with ALENIA (Aeritalia&Selenia), I 10072 Caselle (Torino), Italy.

IEEE Log Number 9144311.

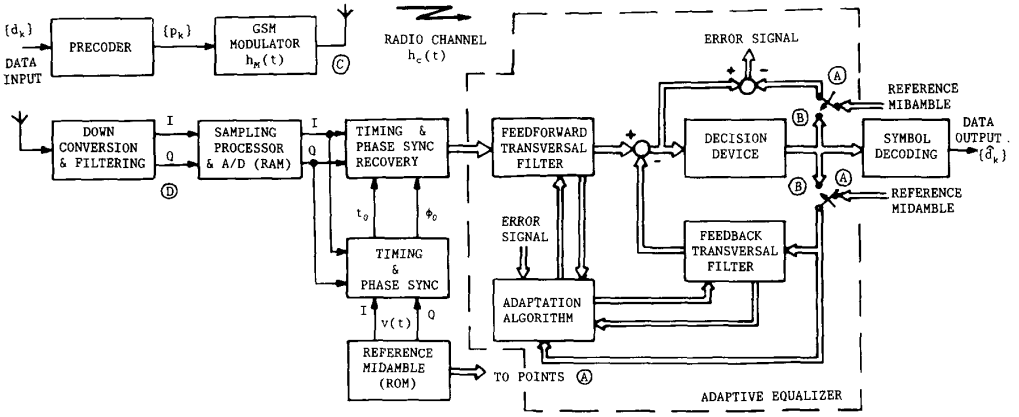

Fig. 2. Block diagram of the simulated system.

TABLE I
SET OF TRAINING SEQUENCES FOR THE CEPT/GSM SYSTEM

Sequence number	Values d_i Decimal	Octal	Hex.	Binary
1	9898135	45604227	970897	00100101110000100010010111
2	12023991	55674267	B778B7	00101101110111100010110111
3	17754382	103564416	10EE90E	01000011101110100100001110
4	18796830	107550436	11ED11E	01000111101101000100011110
5	7049323	32710153	6B906B	00011010111001000001101011
6	20627770	116540472	13AC13A	01001110101100000100111010
7	43999903	247661237	29F629F	10100111110110001010011111
8	62671804	357045674	3BC4BBC	11101111000100101110111100

statistical independence between the current equalizer's input and the previous sets of tap coefficients. In order to cope with such disadvantages, the equalizer adaptation is cast as a classical recursive discrete-time Wiener-Hopf problem: i.e., at every new equalizer input and output it finds the set of equalizer coefficients minimizing the accumulation of the squared errors up to the current time [7]. This approach is referred to as recursive least squares (RLS).

This paper introduces the theoretical aspects and provides the performance evaluation, obtained by computer simulation, of the narrow-band TDMA mobile radio system with RLS equalizers. In particular, the performance is evaluated by bit error rate curves and by the so-called signature curves [14]. The main causes of loss of performance are addressed, i.e., limited time for convergence due to short training sequences, steady-state excess mean square error (MSE) due to the exponential weighting of the squared error sequence and to the non-stationarity of signals, finite-precision arithmetic (also contributing to the excess MSE).

Other topics of interest are the accuracy required to reach the infinite-precision equalizer performance, the length of the digital tapped-delay lines (i.e., number of tap coefficients) necessary to get satisfactory performance.

Hardware complexity is also considered to compare different RLS algorithms, i.e., the standard Kalman, the square root Kalman, the fast Kalman, the LS lattice, and the gradient lattice algorithms, applied to linear transversal equalizers (LTE's), nonlinear decision-feedback equalizers (DFE's), and lattice equalizers (LE's) [4], [7], [9].

The continuous-phase compact-spectrum modulation method recommended by ETSI/GSM [24], with coherent demodulation, is assumed. The four phase shift keying (4PSK) is also considered in some cases for comparison purposes.

II. System Characteristics

The basic time slot of Fig. 1 is assumed, as recommended in [2]. Eight different preamble sequences have been searched for, with good cross-correlation properties in order to reduce the effects of cochannel interference from transmitters using the same carrier frequency in neighboring cells. The chosen sequences (see Table I) also have good properties for the initial training and fast convergence of the adaptive equalizer, as outlined in [6]. One of the sequences used in this paper is 00100101110000100010010111. Only the central 16-b sequence has been selected for suitable correlation properties, while the first and last 5 b have been added to account for the time dispersion of the channel impulse response and the time-jitter of the received signal burst.

Actually, the preamble is placed in the middle of the time slot, and for this reason in the sequel it will be referred to as "midamble." Moreover, the received time slot is completely stored before its processing, and so it is possible to operate the adaptive equalizer on the two parts of the information message using the same training sequence.

The guard time of Fig. 1 has been introduced to avoid overlapping between contiguous bursts.

A. Transceiver

The general block diagram of the simulated system is depicted in Fig. 2. The gross bit rate is 270.8 kb/s. The modulation format adopted by ETSI/GSM [24] is a smoothed minimum shift keying belonging to the 12PM3 class [11]

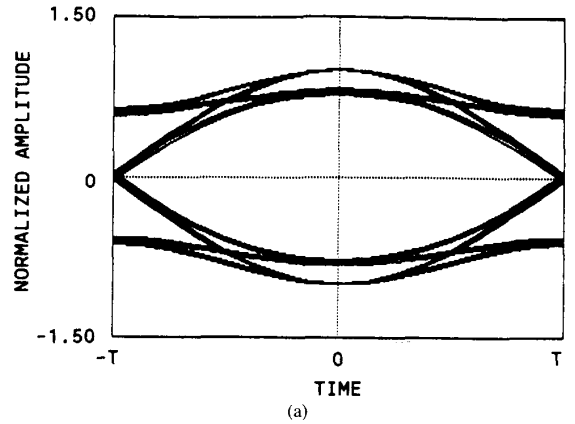

(a)

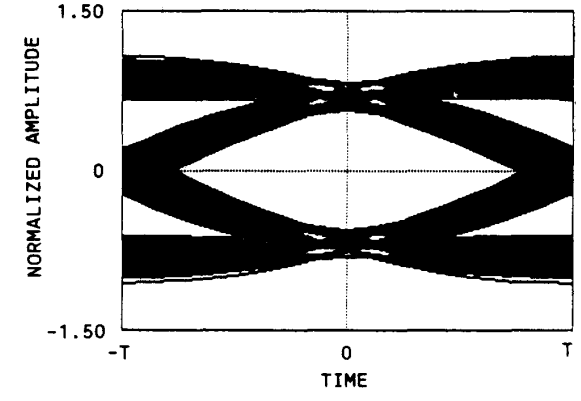

(b)

Fig. 3. In-phase eye-diagram of the transmitted (point C of Fig. 2) and received (point D of Fig. 2) ESTI/GSM signal.

equivalent to a Gaussian minimum shift keying (GMSK) [10], [12], with coherent demodulation. Such a modulation format produces a constant-envelope, compact-spectrum signal suitable for land mobile radio applications.

The parameter characterizing the GMSK modulation is the normalized 3-dB bandwidth BT, where T is the bit period (equal to $1/2$ of a symbol period T_s). All the results presented throughout this work can be referred to $BT = 0.3$.

The in-phase eye-diagram of the transmitted signal (point C of Fig. 2) is depicted in Fig. 3(a); the quadrature eye-diagram is similar, but shifted by T.

The coherent demodulation receiver includes an IF RX filter (ideally equalized seven-pole Butterworth, with 3-dB bandwidth equal to $1.56 f_{\text{bit}} = 1.56/T$) and a BB RX filter (ideally equalized five-pole Butterworth, with 3-dB bandwidth equal to $0.5 f_{\text{bit}} = 0.5/T$).

The in-phase eye-diagram of the undistorted received signal (point D of Fig. 2) is depicted in Fig. 3(b).

Before entering the GMSK modulator, each data value $d_k \epsilon \{0,1\}$ is precoded as

$$p_k = d_k \oplus d_{k-1} \tag{1}$$

where $\oplus$ denotes modulo 2 addition. In this way, at the decision point after the coherent demodulator (point D in Fig. 2), the sampled data value on each branch is uncorrelated with respect to the preceding data values, and so the demodulation process is similar to that performed with an offset-4PSK (OQPSK), except for some sign inversion.

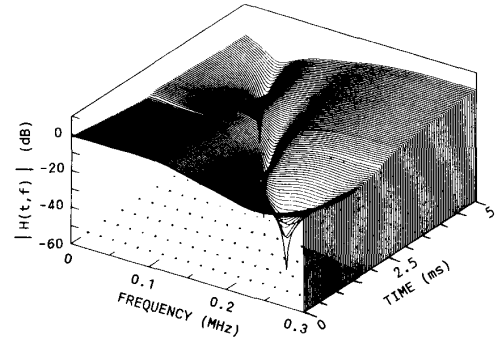

Fig. 4. Example of simulation of the magnitude of the channel transfer function $|(H(t, f))|$.

B. Propagation

To assess the performance of the equalizer structure studied in this paper, we have considered four propagation models, among those of interest of ETSI/GSM.

1) Typical Urban Propagation Model: The propation medium between the base and mobile stations in a typical 900-MHz band urban or suburban environment may be represented by a time- and frequency-dependent channel transfer function $H(t, f)$. This means that the impulse response of the system depends not only on the frequency, but also on time.

At CSELT, research has been performed [13] to give an accurate model for frequency-selective time-dependent multipath channels, using measured data for calibration. A simulation program [13] permits to evaluate the complex transfer function $H(t, f)$, within a bandwidth up to about 8 MHz, for various topographical conditions, different multipath time delay profiles and different Doppler frequency shifts.

An example of simulation of $|H(t, f)|$ is shown in Fig. 4, assuming an exponential power delay profile, representative of a typical urban and suburban mobile radio channel, according to the ETSI/GSM specifications [29], [13]. Each sample of $|H(t, f)|$ lasts 50 μs and is represented within a frequency bandwidth of 300 kHz. The vehicle speed is 50 km/h, the average delay and delay spread are both 1 μs.

The example of Fig. 4 shows that the channel is not time-invariant during the burst transmission.

2) Two-Path Propagation Model: To compare the performance of the system under consideration against that of others presented in the technical literature, each $H(t_i, f)$ of Fig. 4 may be approximated by a simple two-path model, i.e.,

$$H(f) = a - b \cdot \exp\left[-j2\pi(f - f_0)\tau\right] \tag{2}$$

where f_0 is the frequency offset of the notch from the carrier frequency f_c, τ is the relative delay between the two paths, and b is the amplitude of the second path with respect to the amplitude a of the main path. When τ becomes negative, or

$|b| > 1$, the channel enters the so-called nonminimum phase condition.

The values of b, f_0, and τ could be derived from the analysis of each $H(t_i, f)$. However, in this paper we consider the range of τ defined by ETSI/GSM (i.e., 0–16μs), while the values of b and f_0 are those necessary for the computation of the "signature curves" [14]. In fact, the model expressed by (2) allows the system to be characterized by such curves, which are a plot of the critical notch depth $B_c = 20 \cdot \log|1 - b_c|$ that causes outage, when noise is negligible, vs f_0, at a given value of the echo delay τ. The criterion defining outage may be, in the absence of noise, closure of the eye diagram, or reaching a bit error rate threshold. We have verified that the two criteria give substantially the same signature curves.

3) Uncorrelated Rayleigh Two-Path Model: Another model considered in this paper is the uncorrelated Rayleigh two-path model, defined by (2), where a and b are Rayleigh random variables (RV's), whereas f_0 is a uniformly distributed RV. In this case, performance can be assessed through the bit error ratio curves versus the signal-to-noise ratio for specified values of τ and $\alpha = \bar{b}/\bar{a}$, where the overbar denotes the expectation of a RV.

4) Flat Rayleigh Propagation Model: The flat (i.e., single path) Rayleigh time-selective fading channel is characterized by the Doppler frequency shift due to the vehicle movement.

In models 3) and 4) the relationship between the model parameters a and b and the vehicle speed is given by the cutoff frequency of the low-pass filters generating the bandlimited processes a and b: in fact, this cutoff frequency is determined from the Doppler frequency, which is in turn determined from the vehicle speed.

C. Synchronization

To recover the necessary symbol timing and carrier phase of the coherent ETSI/GSM receiver, the correlation properties of suitably designed [11] binary sequences are exploited.

The synchronization strategy adopted in this paper first oversamples (e.g., four samples/bit) the received 26-b midamble sequence $v(t)$ (this is performed by the sampling processor of Fig. 2). Such an oversampling produces K (e.g., $K = 4$ in the case of 4 samples/bit) received midamble sequences $r_i(t)$, $i = 1, \cdots, K$.

Second, K complex correlation functions $R_i(t)$, $i = 1, \cdots, K$, between the corresponding sequences $r_i(t)$ and the complex reference midamble sequence $v'(t)$ are computed. The complex reference midamble $v'(t)$ stored in the receiver (ROM of Fig. 2) is obtained by sampling the 16 central bits of a 26-b MSK-modulated signal. The modulating sequence is formed by the precoded symbols $\{p_k\}$ of Fig. 2. Of course, the in-phase and quadrature components of the so-obtained reference complex midamble are offset by a bit period.

The K magnitudes $A_i(t)$, $i = 1, \cdots, K$ of the correlation functions $R_i(t)$ are then given by

$$A_i(t) = \sqrt{\left[R_i^I(t)\right]^2 + \left[R_i^Q(t)\right]^2} \tag{3}$$

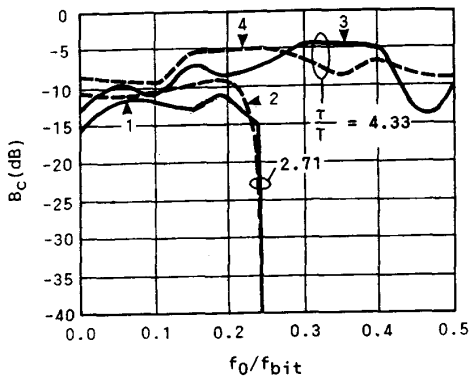

Fig. 5. Comparison among signature curves relevant to the correlation-based synchronization (dashed curves 2 and 4) and to the synchronization method producing zero errors over the simulated sequence (solid curves 1 and 3).

where $R_i^I(t)$ and $R_i^Q(t)$ are the in-phase and quadrature components of $R_i(t)$, respectively.

Third, the sampling instant t_0 is obtained as the peak instant of that $A_i(t)$ with maximum peak value, with a further time shift of $(j-1)T/K$, which takes account of oversampling; j is the value of index i corresponding to that $A_i(t)$ with maximum peak value.

Fourth, the carrier phase rotation φ_0 is given by

$$\varphi_0 = \arctan\left[R_j^Q(t_0)/R_j^I(t_0)\right]. \tag{4}$$

The values of t_0 and φ_0 are affected by an estimation error resulting from the nonoptimum self- and autocorrelation properties and from the additive noise. To check the range of effectiveness of such a synchronization method and the accuracy of t_0 and φ_0, we have compared its performance with that of a second method, based on simultaneous time and phase shiftings of the received signal after the baseband equalizer, until the error counting at the decision point gives zero errors over the simulated sequence. An example is depicted in Fig. 5, which shows a few signature curves computed according to the two described techniques.

III. Adaptive Baseband Equalization

For the considered application, three characteristics are important: fast initial convergence (during the "training phase"), good tracking of the time-varying channel (during the "information" or "tracking phase"), and low computational complexity.

Regarding the first two items, it is known [8], [26], [27] that the RLS algorithms yield significantly faster initial convergence and better tracking in a nonstationary environment than the gradient algorithms (also known as least mean squares (LMS) algorithms). This is particularly true in the case of fading channels varying very rapidly relative to the bit rate (with the ETSI/GSM system, this typically happens in the case of application to high-speed trains, i.e., vehicle speed of the order of 300 km/h or more, as also considered in this paper).

The problem of error propagation has been studied, for example, in [28], where "crashes" (i.e., catastrophic error

propagation) have been observed for decision-directed adaptation during deep fades. To counteract this phenomenon and reconverge within a reasonable time, the receiver's decisions have been replaced, with a certain periodicity [28], by a known data sequence. In the case of the ETSI/GSM system the midamble of 26 b which has a periodicity of about 156 b can be used to this purpose and to restart the equalizer. Such a technique has proved to be very effective and has been taken into account in the presented results.

Moreover, in contrast to the LMS algorithms, the convergence rate of the RLS algorithms is insensitive to the eigenvalue spread of the signal autocorrelation matrix, and when the signal characteristics undergo a step change they converge exponentially and uniformly. This is very important to cope with non-*a priori* known and nonstationary channels.

Hence, the RLS algorithms must be used at least during the short training sequence (26-b long) because of the slow initial convergence properties of the LMS algorithms, as discussed in what follows.

Regarding the third item, as computational complexity we mean the weighted number of operations (additions, multiplications, divisions) that the adaptation algorithm has to perform in a symbol period. With currently available devices, additions and multiplications need about the same computation time, while divisions need dedicated macro-instructions. This implies that the number of divisions M_D is a significant cost parameter, even when the number M_M of additions and multiplications is higher. Moreover, we are interested in computational complexities that allow real-time implementations, using DSP's or dedicated circuitry.

In order to get low-computational complexities, we have initially considered two main classes of algorithms, i.e., the stochastic gradient (SG) and the RLS algorithms. In the first class we have considered the gradient steepest-descent (GSD) and the gradient lattice (GL) algorithms, in the second class the Kalman, fast Kalman (FK), square root Kalman (SRK), and least squares lattice (LSL) algorithms.

With reference to a DFE structure with $L = M + N$ tap coefficients (M and N being the number of feedforward and feedback taps, respectively), Table II [4] and Fig. 6 compare the previously mentioned adaptation algorithms. In the sequel, the DFE structure will be referred to as (M,N)DFE.

It turns out that the least complex algorithm is the GSD, but it is well known that its speed of convergence is too slow (i.e., > 400–500 symbol periods) for our application. Apart from the GSD algorithm, for $4 \leq L \leq 7$ (i.e., the range of our interest), the best method from the M_M standpoint is the SRK, but it requires $2M$ divisions. Similar considerations can be done for the GL and the LSL algorithms. For large values of L the Kalman algorithm is the most complex, but it becomes feasible for low L. The FK algorithm is the least complex for large values of L and has a complexity similar to that of the Kalman algorithm for $4 \leq L \leq 7$.

In conclusion, from the complexity point of view the FK algorithm turns out to be a good solution when the number of tap coefficients cannot be kept less than five because of performance requirements.

Important items that influence the training and tracking

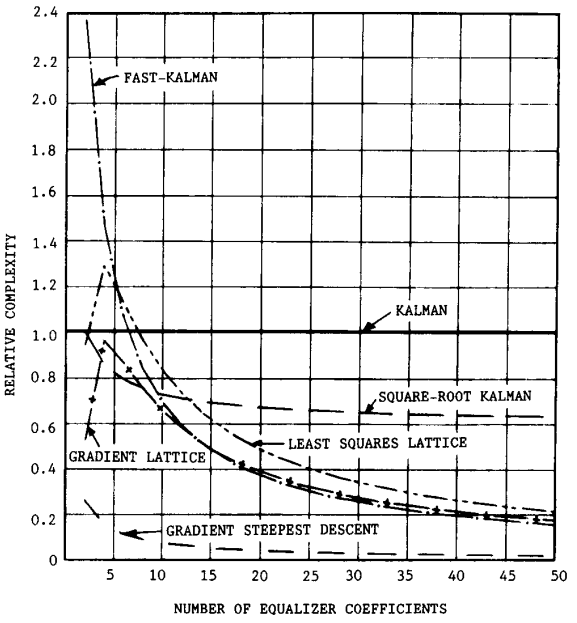

Fig. 6. Number of additions and multiplications of the stochastic gradient and recursive least squares algorithms relative to that of the Kalman algorithm.

TABLE II
COMPUTATIONAL COMPLEXITY OF THE STOCHASTIC GRADIENT AND RECURSIVE LEAST SQUARES ALGORITHMS FOR A DECISION FEEDBACK EQUALIZER WITH M FEEDFORWARD TAPS AND N FEEDBACK TAPS $L = (M + N)$

Adaptation Algorithm	Number of Additions and Multiplications	Number of Divisions
Gradient steepest-descent	$2L + 1$	0
Kalman	$2.5L^2 + 4.5L$	2
Fast-Kalman	$20L + 5$	3
Square-root Kalman	$1.5L^2 + 6.5L$	L
Least squares lattice	$18M + 39N - 39$	$2M$
Gradient lattice	$13M + 33N - 36$	$2M$

behaviors of adaptive equalizers with the FK algorithm are: i) the exponential windowing for the autocorrelation matrix estimate, ii) the filtering of nonstationary signals (typical in a mobile radio environment), and iii) the excitation properties of the training signal and the initial convergence.

Besides these topics, we are also interested in considering the implementation in finite-precision arithmetic.

In what follows, a description of the basic principles and equations of the complex adaptive equalizer with the FK algorithm, called *complex FK algorithm* (CFKA), is presented. The mathematical details are given in [7], [17].

A. Adaptation Algorithm

In this section a description of the equalizer structure and a brief review of the adaptation algorithm are presented. The criteria for the design of the main adaptation parameters are also given.

The decision feedback equalizer of Fig. 7 consists of two branches (because of the quadrature-type modulation), each

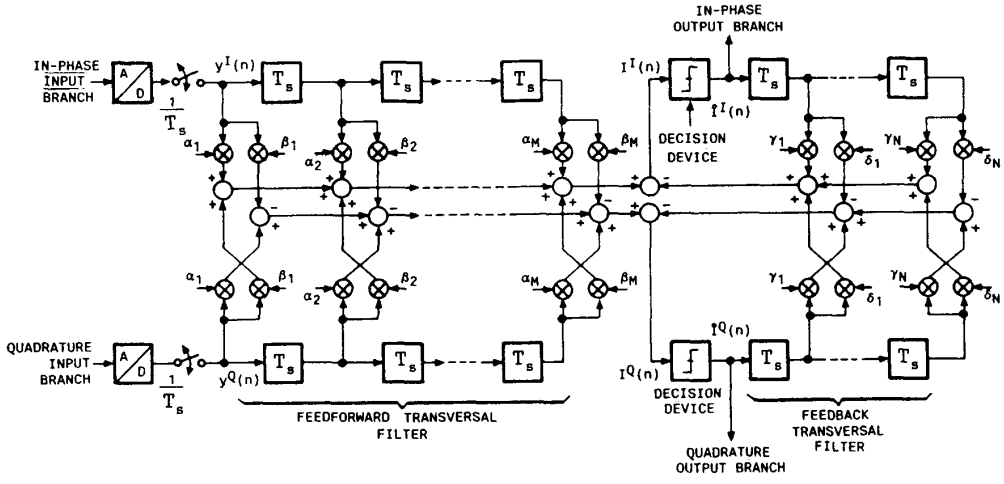

Fig. 7. Block diagram of the decision-feedback equalizer.

with a feedforward and a feedback section. The feedforward and the feedback sections are linear transversal filters with M and N complex tap coefficients, respectively.

In this paper, we have assumed a tap spacing equal to T_s, but it is worth noting that a tap spacing smaller than T_s ("fractional tap spacing") can lead to better performance of the equalizer in the presence of symbol timing estimation errors.

Notice that during the initial equalizer training period (switch on position A in Fig. 2), a succession of data symbols $D(0), D(1), \cdots, D(n)$ known by the equalizer adaptation algorithm and stored in its control unit is transmitted over the channel, resulting in a sequence of equalizer inputs $y(0), y(1), \cdots, y(n)$.

During the training period, the equalizer complex output at time n $I(n)$ differs from the ideal output $D(n)$ by an error $e(n)$

$$e(n) = D(n) - I(n) \tag{5}$$

Let $\hat{I}(n)$ be an estimate of the nth transmitted symbol and $\hat{I}(n-1) \cdots \hat{I}(n-N)$ the previously detected symbols (the decision $\hat{I}(n)$ is formed by quantizing the equalizer complex output $I(n)$ to the nearest information symbol). Then, during the tracking period (switch on position B in Fig. 2) the error $e(n)$ is replaced by

$$\hat{e}(n) = \hat{I}(n) - I(n) \tag{6}$$

Now, assuming that previously detected symbols in the feedback section are correct (and no propagation error arises), (6) can be replaced by $\hat{e}(n) = i(n) - I(n)$ in the mathematical derivation of the adaptation algorithm, $i(n)$ being the transmitted information symbol at time n.

The minimum mean square error (MMSE) criterion provides a practical means for designing the feedforward and feedback equalizer coefficients $\{c_M(n)\}$ and $\{d_N(n)\}$, respectively. It minimizes the mean square errors at time n

$$\epsilon_1 = E\left\{\left[D(n) - I(n)\right]^2\right\}, \tag{7}$$

$$\epsilon_2 = E\left\{\left[i(n) - I(n)\right]^2\right\}, \tag{8}$$

during the training and tracking periods, respectively.

The minimization of (7) or (8) leads to a set of linear equations for the tap coefficients, whose theoretical values can be computed exactly if the values of signal and noise variances and the channel impulse response are known. See, for example, [15] and [16] for an analytical derivation of the theoretical coefficients. The calculation of the theoretical coefficients is primarily useful in providing a baseline performance for comparison against the actual adaptation schemes.

Instead of minimizing the MSE of (7) and (8), the LS algorithms minimize an exponentially weighted squared error at time n, i.e.,

$$J(n) = \sum_{h=0}^{n} \lambda^{n-h}\left[D(h) - \boldsymbol{Y}_L^*(h) \cdot \boldsymbol{C}_L(h)\right]^2 \tag{9}$$

where $\boldsymbol{Y}_L(h)$ is the overall complex input sequence (of dimensionality $L = M + N$), fed to the feedforward and feedback sections of the equalizer; $\boldsymbol{C}_L(n)$ is the overall (i.e., feedforward and feedback) equalizer complex coefficient vector (of dimensionality L); the superscript asterisk denotes complex conjugate transposed matrix or vector; λ is a positive number close to, but less than 1. The quantity $1/(1-\lambda)$ is the "memory" of the algorithm.

The RLS algorithms have been developed to solve recursively in time the Wiener–Hopf equation which provides the minimizing vector $\boldsymbol{C}_L(n)$ for (9).

The recursive operation of the CFKA for the time-update of the set of coefficients $\boldsymbol{C}_L(n)$ proceeds as described in [7], [17]. The resulting time-update relationship for the equalizer coefficients, i.e.,

$$\boldsymbol{C}_L(n) = \boldsymbol{C}_L(n-1) + \boldsymbol{K}_L(n) \cdot e^*(n) \tag{10}$$

highlights that the rapid convergence of the Kalman algorithm is due to the control applied to each tap coefficient through a corresponding element of the L-dimensional Kalman gain vector $\boldsymbol{K}_L(n) = \boldsymbol{P}_{LL}(n) \cdot \boldsymbol{Y}_L(n)$. In the channel

matrix $\boldsymbol{P}_{LL}(n)$, defined as

$$\boldsymbol{P}_{LL}(n) = \left[\sum_{h=0}^{n} \lambda^{n-h} \boldsymbol{Y}_L^*(h) \cdot \boldsymbol{Y}_L(h) + \delta\lambda^n \boldsymbol{I}_{LL}\right]^{-1} \quad (11)$$

it is worth noting the presence of the second parameter δ, which is a small positive constant to ensure nonsingularity and turns out to be an estimate of the final MSE [4], [7]. Furthermore, $\boldsymbol{P}_{LL}(n)$ performs the appropriate orthogonalization of the autocorrelation matrix, and so greatly accelerates the adaptation process [8].

In computing the equalizer coefficients through (10), an estimation error $\Delta\boldsymbol{C}_L(n) = \boldsymbol{C}_L(n) - \boldsymbol{C}_{\text{opt}}$ is made with respect to the optimum coefficients $\boldsymbol{C}_{\text{opt}}$. Such an error is reflected on a misadjustment MSE $\Delta\epsilon_1$ above the minimum MSE $\epsilon_{\min}$.

The best steady-state performance is obtained for $\lambda = 1$ (i.e., infinite system memory) and corresponds to a nontracking situation. As the memory of the system decreases ($\lambda \to 0$), faster tracking is obtained, at the cost of increased misadjustments $\Delta\epsilon_1$ and $\Delta\boldsymbol{C}_L$.

When the input signal is non-stationary, the quantities involved in the Wiener–Hopf equation computing the optimum coefficients $\boldsymbol{C}_{\text{opt}}(n)$ are functions of time. The estimation algorithm tracks the channel variations with a lag dependent only on its time constant, that is, its memory, irrespectively of the type of channel.

In this case increasing λ produces a further increase (called lag MSE $\Delta\epsilon_2$) of the excess MSE and the algorithm cannot track variations of the input statistics.

In conclusion, a trade-off between the two requirements (i.e., $\lambda \to 1$ to reduce $\Delta\epsilon_1$ and $\lambda \ll 1$ to reduce $\Delta\epsilon_2$) has to be searched for. In this paper the optimization of λ has been performed by computer simulation of different system conditions.

B. Initial Convergence and Training Sequences

The Kalman-type algorithms feature a high speed of convergence (meant in the sense of $\epsilon = 1.5\epsilon_{\min}$ [20]) that allows good equalizer coefficient estimates in a time period less or equal to $2L$ (in the absence of noise or for high values of signal-to-noise ratios). This is an outstanding property when the system, as discussed in Section II, can use training sequences of only 26 b.

One of the purposes of this paper was to verify, by computer simulation, the actual convergence properties of the Kalman-type algorithms over the ETSI/GSM mobile radio channels.

It can be shown [20] that for large values of n the MSE can be written as

$$\begin{aligned}\epsilon &= \left[\epsilon_{\min} \cdot \text{trace}(\boldsymbol{I}_{LL})\right]/(n-1) + \epsilon_{\min} \\ &= \epsilon_{\min}\left[1 + L/(n-1)\right] \end{aligned} \quad (12)$$

where $\boldsymbol{I}_{LL}$ is the identity matrix.

From (12) we note that the MSE convergence (i.e., $\epsilon = 1.5\epsilon_{\min}$) is attained after about $2L$ iterations. In Section IV-A we estimate by simulation the number of iterations in the case of a few ETSI/GSM mobile radio channels.

Fast convergence is obtained if the training signal makes the matrix $\hat{\boldsymbol{R}}_{LL}(n)$, involved in the Wiener-Hopf equation for the computation of the equalizer coefficients, be positive definite. In fact, in this case, the cost function (9) defines a hypersurface (a paraboloid) in an L-dimensional space, with only one minimum. If the signal to be equalized is not stationary, such a surface drifts over time, and defines, with its minimum, the set of optimum coefficients; however, the Kalman algorithm can still attain a fast convergence to the minimum point.

Since $\hat{\boldsymbol{R}}_{LL}(n)$ can be written as

$$\hat{\boldsymbol{R}}_{LL}(n) = \sum_{h=0}^{n} \lambda^{n-h} \boldsymbol{Y}_L(h) \cdot \boldsymbol{Y}_L^*(h) \quad (13)$$

the condition $\det(\hat{\boldsymbol{R}}_{LL}(n)) \neq 0$ implies the matrix $[\boldsymbol{Y}_L(0) \cdots \boldsymbol{Y}_L(n)]$ be of rank L. This is true if the signal that produces the matrix $[\boldsymbol{Y}_L(0) \cdots \boldsymbol{Y}_L(n)]$ is periodic in the time domain (with at least L spectral lines in the frequency domain). In fact, it is well-known [30] that the eigenvalues of circulant matrices are determined by the discrete Fourier transform of the first row, which is formed by samples of the periodically repeated channel impulse response. Consequently, the matrix $[\boldsymbol{Y}_L(0) \cdots \boldsymbol{Y}_L(n)]$ has full rank L provided that the discrete Fourier transform of the periodically repeated channel impulse response has no zero values. The signal $y(k)$ that produces the matrix $[\boldsymbol{Y}_L(0) \cdots \boldsymbol{Y}_L(n)]$ and satisfies such a condition is said to be sufficiently rich; for a system of order $L/2$, the following $y(k)$ signal becomes sufficiently rich:

$$\begin{aligned} y(k) &= \sum_{i=1}^{m} \mathcal{A}_i \sin\left(2\pi k f_i T\right), \\ f_1 < f_2 < \cdots < f_m, &\qquad m \geq L/2;\ T < 2f_{L/2}. \end{aligned} \quad (14)$$

The signal $y(k)$ can be obtained by sampling the continuous signal

$$y(t) = \sum_{i=1}^{m} \mathcal{A}_i \sin\left(2\pi f_i t\right) \quad (15)$$

which contains more than $L/2$ frequencies, with time interval T.

This criterion has been followed to choose good training sequences, even though our signal is not periodic because only one training sequence and not a periodic repetition of it can be used during the training phase. However, we have verified by computer simulation that it is possible to obtain, with the assumed channel characteristics, initial convergence times close to the theoretical value $2L$ also when the training sequence is made of a single repetition, provided that its spectrum is large enough in the useful bandwidth. Eight training sequences satisfying the above-described criterion are reported in Table II.

Finally, it has to be remarked that also the information signal of the basic time slot should have spectral content such that $\det(\hat{\boldsymbol{R}}_{LL}(n)) \neq 0$. This is a very important constraint, which can be fulfilled by scrambling the transmitted signal through a pseudorandom sequence.

C. Implementation in Finite-Precision Arithmetic

All the algorithms of the RLS family have impaired performance when implemented using finite-precision arithmetic for the representation and calculation of the involved variables. In particular, errors due to reduced computational accuracy impair the adaptation of the signal autocorrelation matrix, whose elements are computed as sum of the current equalizer inputs with the weighted previous inputs. This produces error accumulation and, in some cases, algorithm instability, unless proper countermeasures are adopted.

As shown by [22], the Kalman and SRK algorithms are exponentially stable [21] if the elements $[\hat{\boldsymbol{R}}_{LL}(n)]^{-1}$ are not very large (i.e., when the autocorrelation signal matrix $\hat{\boldsymbol{R}}_{LL}(n)$ is not close to a singular matrix) and $\lambda < 1$. If $\lambda = 1$ they are only asymptotically stable.

If $\lambda < 1$, as usually assumed for tracking reasons, it can be shown [22] that the Kalman algorithm is stable provided that binary words of at least 16 bits are used to reduce the effect of the several sources of errors.

The SRK algorithm is stable using binary word lengths of 10 to 15 bits, provided that a Levinson–Durbin decomposition is used for the adaptation of $[\hat{\boldsymbol{R}}_{LL}(n)]^{-1}$.

The lattice-type algorithms are always stable using binary word lengths of at least 8 b.

The FK algorithm is stable only if $\lambda = 1$. It shows instability after a time period that shortens as λ and the length of the binary words (a minimum of 10 b seems to be necessary [22]) decrease. However, when such an instability has not yet arisen and when the number of bits is in the range 10–15, this algorithm gives better numerical accuracy (i.e., a smaller estimation error for the same amount of roundoff error) than the Kalman, SRK, and LSL algorithms [22]. Consequently, in order to exploit the characteristics of the FK algorithm discussed above, it is very convenient to adopt some sort of restarting procedure, i.e., a periodic reinitialization of the algorithm to avoid the build-up of roundoff errors with time.

Several restarting procedures have been proposed in the literature [8], [17], [23]. In our narrow-band TDMA mobile radio application, since we are already working with a burst transmission structure, a particular restarting procedure is not necessary. In fact, the presence of a training sequence in each time slot allows a complete algorithm reinitialization and the channel burst duration is shorter than the period of time after which instability arises.

In conclusion, we have verified by simulation that a FK algorithm implementation with a 16-b DSP without restarting procedures is feasible for a narrow-band TDMA mobile radio system.

IV. Performance Results

The results of this section have been obtained using a computer simulation program developed at CSELT.

In the sequel, we discuss the following aspects of the performance of adaptive LTE's and DFE's with the CFKA: 1) initial convergence and steady-state behavior of the adaptation algorithm; 2) distortion compensation capability, studied through the use of the signature curves; 3) bit error ratio (BER) versus the energy-per-bit to noise-spectral-density ratio E_b/N_0 in the presence of thermal noise and multipath fading distortions; 4) required accuracy (in terms of number of bits) of the A/D converter at the equalizer input, of the tap coefficients, and of the adaptation process.

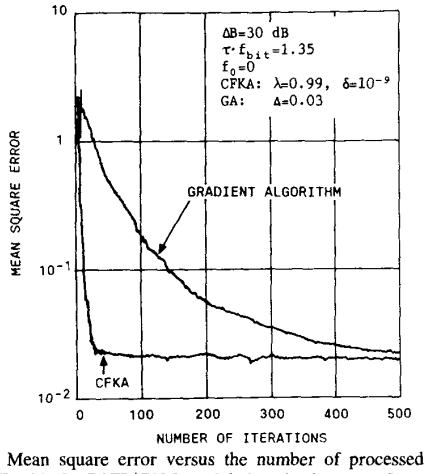

Fig. 8. Mean square error versus the number of processed bits for the (2, 3)DFE with the ESTI/GSM modulation, in the case of a step transition from a flat channel to a two-path channel with $B = -30$ dB, $\tau \cdot f_{\text{bit}} = 1.35$, $f_0 = 0$.

A. Initial Convergence and Steady-State Behavior

As discussed in Section III-B, fast initial convergence needs an "optimum" training sequence. The results presented throughout refer to the sequence already introduced in Section II, i.e., 00100101110000100010010111. Remember that the TDMA system requires that the convergence time be roughly finished by the end of the training phase.

Fig. 8 shows the MSE versus the number of processed bits for a (2, 3)DFE and the ETSI/GSM modulation, in the case of a two-path propagation model (model *b* in Section II-B) when a step-variation of 30 dB is applied to the value of the notch level B, with the specified values of echo delay and notch frequency offset, starting from a "flat" channel. (As shown in Section IV-B, the (2, 3)DFE turns out to be a good solution from the complexity and performance points of view.) The plots show that the GSD algorithm converges slowly on this channel, i.e., after about 500 iterations with $\Delta = 0.03$ (convergence is meant in the sense of (12), i.e., $\epsilon = 1.5\epsilon_{\min}$). In contrast, the CFKA has a rapid convergence time, i.e., about 20 iterations: this is twice the theoretical minimum convergence time of $2L = 10$ iterations, as discussed in Section III-B. In Fig. 8 the weighting factor λ is 0.99, the constant δ is 10^{-9}. Moreover, notice that the GSD algorithm exhibits a greater excess MSE than the CFKA. For the latter the excess MSE corresponds to the value of (12).

Fig. 9 depicts the time behavior of the real parts of the 5 complex coefficients of the (2, 3)DFE with CFKA and the ETSI/GSM modulation, as a response to the previously described channel variation. Also marked are the theoretical values. Fig. 10 gives the real parts of 5 complex coefficients of a LTE in the same situation of Fig. 9. It is worth noting that the adaptation process is well completed within the 26-b

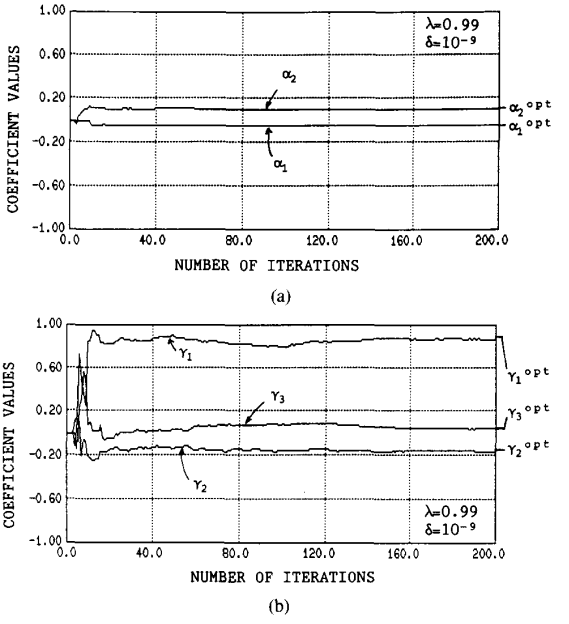

Fig. 9. Real parts of two feedforward (a) and three feedback (b) coefficients of the (2, 3)DFE with the CFKA. Step transition from a flat channel to a two-path channel with $B = -30$ db, $\tau \cdot f_{bit} = 1.35$, $f_0 = 0$. ETSI/GSM modulation; coherent demodulation. $\alpha_1^{opt} = -0.0478$; $\alpha_2^{opt} = 0.109$; $\gamma_1^{opt} = 0.894$; $\gamma_2^{opt} = -0.156$; $\gamma_3^{opt} = 0.0473$.

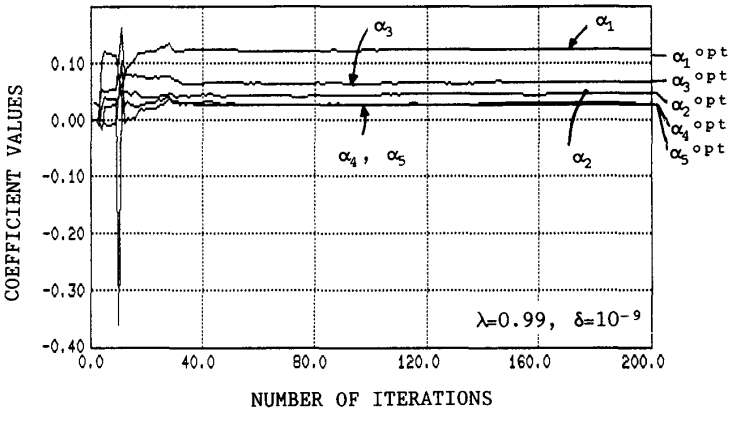

Fig. 10. Real parts of the five coefficients of a linear transversal equalizer with the CFKA. Step transition from a flat channel to a two-path channel with $B = -30$ dB; $\tau \cdot f_{bit} = 1.35$; $f_0 = 0$. ETSI/GSM modulation; coherent demodulation. $\alpha_1^{opt} = 0.116$; $\alpha_2^{opt} = 0.045$; $\alpha_3^{opt} = 0.065$; $\alpha_4^{opt} = 0.028$; $\alpha_5^{opt} = 0.027$.

long training period. The time behavior of the imaginary parts of the equalizer coefficients turns out to be similar.

B. Distortion Compensation Capability

Each point of the signature curves presented throughout has been computed by applying a step transition (at the beginning of each burst) from the undistorted ("flat") channel to a two-path channel, as defined in Section II-B, with the parameter values specified by the signature point itself. Then the channel is kept constant for the whole burst duration.

Fig. 11 shows the signature curves of the system with the ETSI/GSM parameters, without adaptive equalization and with a symbol timing and phase synchronization producing zero errors over the simulated sequence at the decision point. Notice that the value $\tau f_{bit} = 4.33$ corresponds, with $f_{bit} = 270.8$ kb/s, to the maximum echo delay of 16 μs that the mobile radio system has to cope with, according to the ETSI/GSM working assumption.

As already discussed in Section II-C, Fig. 5 compares the signatures of Fig. 11 for $\tau f_{bit} = 2.71$ and for $\tau f_{bit} = 4.33$ to those obtained by using the correlation-based synchronization.

Fig. 12 shows the same signatures of Fig. 11 in the presence of a linear transversal equalizer with five complex

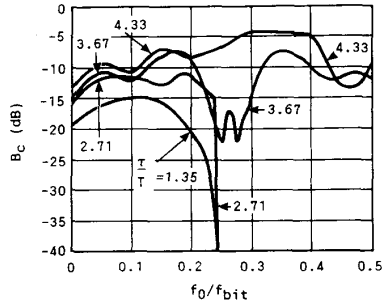

Fig. 11. Signature curves of the system without adaptive equalization for several values of echo delay $\tau \cdot f_{bit}$. Case of symbol timing and phase synchronization technique producing zero errors over the simulated sequence.

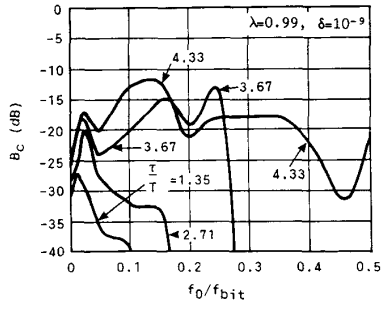

Fig. 12. Signatures of the linear transversal equalizers with five complex coefficients adapted according to the CFKA. Case of symbol timing and phase synchronization technique producing zero errors over the simulated sequence. The corresponding signatures of the (2, 3)DFE are below the −40-dB level.

coefficients and adapted according to the CFKA. In the same conditions we have found that a (2, 3)DFE is able to keep the signature curves below the −40-dB level, and for this reason they do not appear in Fig. 12. Moreover, we have found that this is the simplest DFE structure that provides such a result.

C. Bit Error Rate (BER) Performance

The BER performance of the ETSI/GSM system over the additive white Gaussian noise (AWGN) channel and over the two-path channel is summarized in Figs. 13 and 14. The channel parameters are specified in the caption of Fig. 13. In particular, Fig. 13 shows the BER curves without equalization, together with the reference performance in the presence of AWGN only, and Fig. 14 shows the improvement given by the use of a (2, 3)DFE.

For the undistorted channel, the correlation-based synchronization technique degrades the E_b/N_0 ratio by about 1 dB at BER = 10^{-2}, which is assumed by ETSI/GSM as a quality threshold. In Fig. 14 we report only one BER curve for each synchronization technique because the curves relevant to the four different $\tau \cdot f_{bit}$ values are indistinguishable.

Fig. 15 gives the performance over the uncorrelated two-path Rayleigh (time- and frequency-selective) channel (model *c* of Section II-B) and over the flat-Rayleigh (time-selective) channel (model *d*), considering a (2, 3)DFE. It is worth noting that the equalizer works better when there is time dispersion on the channel (i.e., frequency-selective distor-

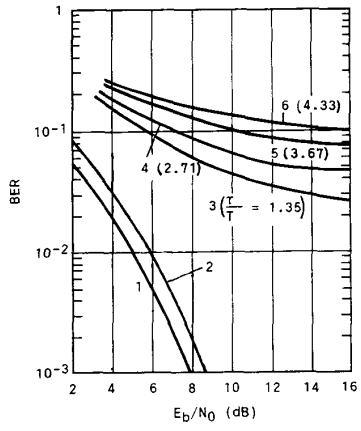

Fig. 13. BER performance without adaptive equalization. (1) Undistorted channel; (2) Undistorted channel, correlation-based synchronization; (3) Two-path channel ($B = -15$ dB, $\tau \cdot f_{bit} = 1.35$, $f = 0$), correlation-based synchronization; (4) As in (3), but for $\tau \cdot f_{bit} = 2.71$; (5) As in (3) but for $\tau \cdot f_{bit} = 3.67$; (6) As in (3) but for $\tau \cdot f_{bit} = 4.33$.

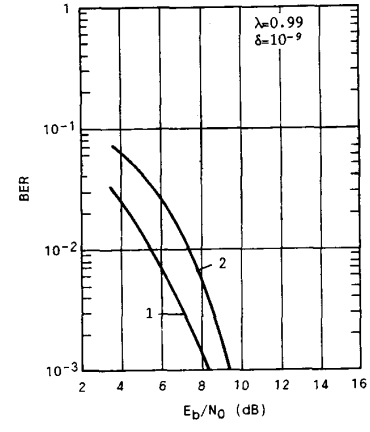

Fig. 14. BER performance with the (2, 3)DFE, in the case of the two-path channel (same parameters as in Fig. 13, with $\tau \cdot f_{bit} = 1.35$–4.33). (1) Symbol timing and phase synchronization technique producing zero errors over the simulated sequence. (2) Correlation-based synchronization.

tions) compared to a flat Rayleigh channel. This means that the two-path channel provides a sort of diversity function.

In addition, always in the case of model *c*, Fig. 16 shows the BER versus the relative echo delay when the E_b/N_0 ratio is 14 dB. The (2, 3)DFE with CFKA can keep the BER less than 10^{-2} for the whole range of specified values of τ, i.e., $0 \div 16$ μs (note that for $\tau = 0$ μs the figure is also relevant to model *d*). For such a value of E_b/N_0 this remains true also for high vehicle speeds, i.e., up to about 300 km/h. The (2, 3)DFE is the simplest DFE structure capable of producing such a performance.

For the BER values of Figs. 13–16 the number of simulated bits was about 2 000 000.

Finally, Fig. 17 presents the BER performance of the (2, 3)DFE over the typical urban channel (model *a*) according to the ETSI/GSM specifications [29]. In this case, the propagation characteristic modeling technique introduced in Section II-B [13] provides a set of time- and frequency-de-

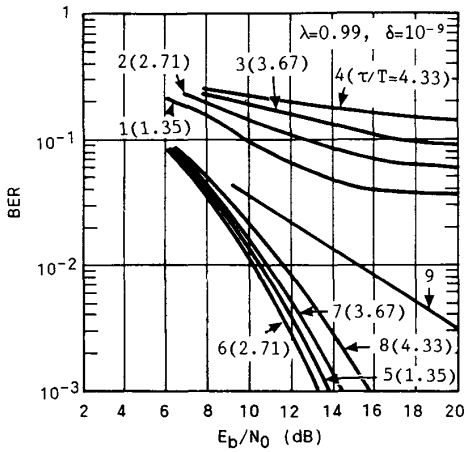

Fig. 15. BER performance. (1)–(4) Two-path Rayleigh channel, $\alpha = 1$, $v = 50$ km/h, correlation-based synchronization. (5)–(8) As (1)–(4), but with the (2, 3)DFE. (9) Flat Rayleigh channel, $v = 50$ km/h, correlation-based synchronization, with (2, 3)DFE.

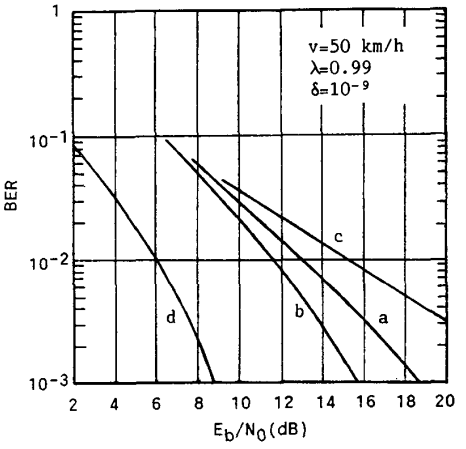

Fig. 17. BER performance with the (2, 3)DFE, in the case of (a) ETSI/GSM typical urban channel. (b) Uncorrelated two-path Rayleigh channel ($\tau \cdot f_{bit} = 4.33$, $\alpha = 1$). (c) Flat Rayleigh channel. (d) Undistorted AWGN channel.

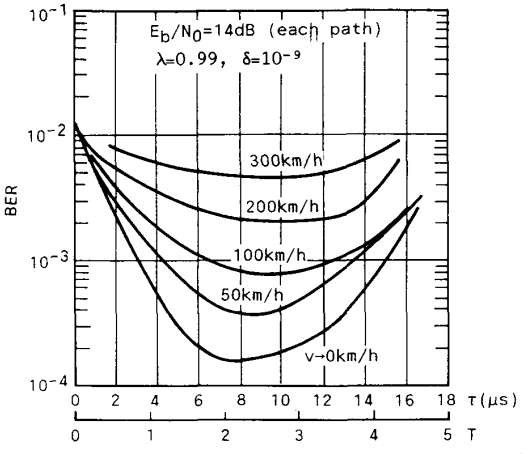

Fig. 16. BER versus the relative echo delay in the two-path Rayleigh channel, correlation-based synchronization and (2, 3)DFE.

pendent linear filters $\{H_i(t, f)\}_{i=1}^{M}$ (see Fig. 4); the number of $H_i(t, f)$ affecting a given time slot depends on the vehicle speed v. For example, when $v = 50$ km/h eleven different $H_i(t, f)$ have to be considered per every time slot. This means that each $H_i(t, f)$ "covers" $156.25/11 = 14.2$ b during which the channel transfer function is meant to be time-invariant.

Consequently, the DFE using the CFKA is "trained" according to the channel characteristics corresponding to the central filters $H_i(t, f)$, but it will have to equalize the channel distortions corresponding to the preceding and to the following $H_i(t, f)$. The same operation is repeated in the following time slots, by considering different sets of eleven $H_i(t, f)$. Moreover, since the signal bursts are transmitted within a TDMA frame with eight time slots, as specified in [2], the sets of consecutive filters $H_i(t, f)$ are drawn from $\{H_i(t, f)\}_{i=1}^{M}$ with the same time periodicity.

Our simulation program, which is frequency-domain based, builds up the distorted bit sequence of the basic time slot by performing eleven (in the case of $v = 50$ km/h) filterings of the modulated signal through eleven $H_i(t, f)$ and by joining the pertaining 14.2 b in the right order. This operation has to be repeated for a number of times large enough to get the statistical completeness required to evaluate the BER values of Fig. 17. For example, when $v = 50$ km/h we have simulated a transmission of about 10 s, corresponding to processing about 190 000 $H_i(t, f)$ and 2 700 000 b.

For the sake of comparison, in Fig. 17 there are also the BER curves of the (2, 3)DFE with the CFKA in the cases of channel models c (for echo delay $\tau / T = 4.33$) and d, taken from Fig. 15. Such a comparison can be useful to evaluate the approximation introduced by the simplified channel models and to design the necessary equalizer size. From the results of Figs. 12 and 14–17 the (2, 3)DFE turns out to be a viable solution.

D. Quantization and Processor Accuracy

From the hardware implementation point of view it is important to keep the number of bits representing the signal samples fed to the adaptive equalizer, the equalizer coefficients, and the arithmetic of the adaptation processor as small as possible. Regarding this last point, in Section III-D we have remarked that for the narrowband TDMA system with channel bursts of 148 b, which has a sort of "built in" restarting procedure, a minimum of 10 b seems to be sufficient for the binary words. In practice we have simulated the CFKA by a 16-bit DSP.

As to the accuracy of the A/D converter at the equalizer input and of the coefficient values, we have tested the equalizer performance when 6-, 8-b, and infinite accuracy have been assumed. Figs. 18 and 19 show the effect of 6- and 8-b accuracy for both the A/D converter and the tap coefficients, considering the 4PSK modulation as an example. It has been found that the dominant cause of degradation is the equalizer coefficient accuracy, while the A/D converter accuracy is not a critical item, as long as a minimum of 6 b is used.

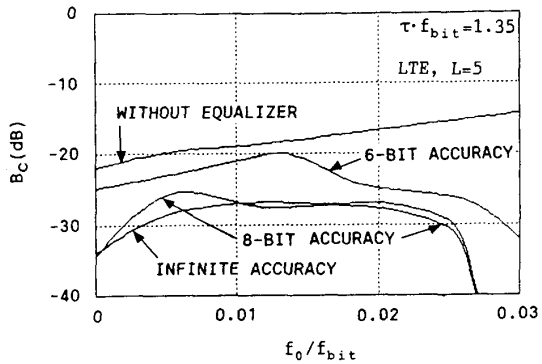

Fig. 18. Effect of finite accuracy of the A/D converter on the signatures of a 4PSK system with five-coefficient LTE.

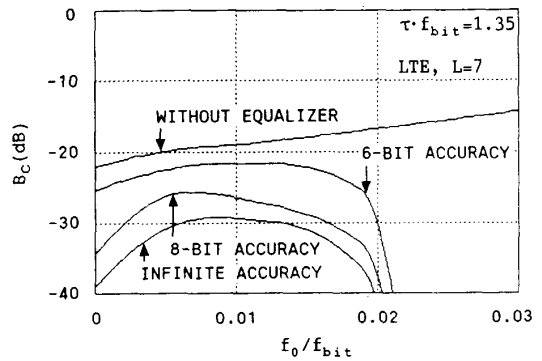

Fig. 19. Effect of finite accuracy of the A/D converter on the signatures of a 4PSK system with seven-coefficient LTE.

V. Conclusions

This paper has shown that an adaptive equalizer is essential for a narrowband TDMA system with the ETSI/GSM characteristics working in a digital cellular mobile radio environment. In particular, four propagation models have been considered, i.e., the ETSI/GSM typical urban channel, the fixed two-path channel, the uncorrelated two-path Rayleigh channel, and the flat Rayleigh channel.

Linear transversal and nonlinear decision feedback equalizers are feasible solutions to cope with the very fast varying frequency-selective distortions, provided that a Kalman-type adaptation algorithm is used to ensure a fast (i.e., within the 26-b long training phase) equalizer coefficient convergence to the steady-state values, and a rapid tracking of the channel variations. This has been checked over the ETSI/GSM typical urban channel, the uncorrelated two-path Rayleigh channel, and the flat Rayleigh channel.

To reduce the computation burden the complex FK algorithm can be used.

In the case of uncorrelated two-path Rayleigh channel, we have found that the (2, 3)DFE with the complex fast Kalman algorithm can keep the BER less than 10^{-2}, which is assumed by ETSI/GSM as a quality threshold, for the whole range of specified values of echo delay, i.e., $0 \div 16$ μs. For a value of E_b/N_0 of at least 14 dB this remains true also for high vehicle speeds, i.e., up to about 300 km/h.

The length of 26 b, fixed by the ETSI/GSM for the training sequence, is sufficient, provided that such a sequence is optimized according to the criterion mentioned in this paper.

Symbol timing and carrier phase must be recovered before performing the adaptation process. A synchronization technique based on correlation processes over the 26-bit training sequence involves a performance degradation in terms of signal-to-noise ratio of about 1 dB at BER = 10^{-2}, with respect to the reference performance on an AWGN channel.

It has been found that a complex decision feedback equalizer with five taps is capable of reducing the signature curves (used to describe the system behavior in the case of fixed two-path channels) below the -40-dB level over the whole range of echo delay values specified by ETSI/GSM. Also the BER curves (computed for the four propagation models considered in this paper) are greatly improved for the whole range of echo delay values.

Finally, for an almost complete reduction of the performance degradation due to the limited accuracy of the A/D converters at the equalizer inputs and of the equalizer coefficients, a binary wordlength of at least 8 b is necessary, whereas the arithmetic of the CFKA requires an accuracy of at least 10 b.

References

[1] "Status of studies, experiments and harmonization process in Europe," technical session in *Proc. Int. Conf. on Digital Land Mobile Radio Communications*, Venice, Italy, June 30–July 3, 1987.

[2] European Telecommunications Standards Institute (ETSI), Rec. ETSI/GSM 05.02, 1990.

[3] W. C. Jakes, Jr., *Microwave Mobile Communication*. New York: Wiley, 1974.

[4] J. G. Proakis, *Digital Communications*. New York: McGraw-Hill, 1989.

[5] G. Ungerboeck, "Adaptive maximum-likelihood receiver for carrier modulated data transmission systems," *IEEE Trans. Commun.*, vol. COM-22, pp. 624–636, May 1974.

[6] G. D'Aria and V. Zingarelli, "Adaptive baseband equalizers for narrowband TDMA/FDMA mobile radio systems," in *Proc. Int. Conf. on Digital Land Mobile Radio Communications*, Venice, Italy, pp. 280–289, June 30–July 3, 1987.

[7] D. D. Falconer and L. Ljung, "Application of fast Kalman estimation to adaptive equalization," *IEEE Trans. Commun.*, vol. COM-26, pp. 1439–1446, Oct. 1978.

[8] E. Eleftheriou and D. D. Falconer, "Tracking properties and steady-state performance of RLS adaptive filter algorithms," *IEEE Trans. Acoust., Speech, Signal Processing*, vol. ASSP-34, pp. 1097–1109, Oct. 1986.

[9] F. Ling and J. G. Proakis, "Adaptive lattice decision-feedback equalizers—Their performance and application to time-variant multipath channels," *IEEE Trans. Commun.*, vol. COM-33, pp. 348–356, Apr. 1985.

[10] K. Murata and K. Hirade, "GMSK modulation for digital mobile radio telephony," *IEEE Trans. Commun.*, vol. COM-29, pp. 1044–1050, July 1981.

[11] M. Quacchia and V. Zingarelli, "An analytical evaluation of bit error probability in mobile radio systems with 12PM3 modulations," *IEEE Trans. Veh. Technol.*, vol. VT-37, pp. 135–150, Aug. 1988.

[12] G. D'Aria, F. Muratore, and V. Palestini, "Performance of GMSK and comparisons with the modulation methods of the 12PM3 class," in *Proc. IEEE Veh. Technol. Conf.*, Tampa, FL, June 1–3, 1987, pp. 246–252.

[13] G. D'Aria, L. Stola, and V. Zingarelli, "Modelling and simulation of the propagation characteristics of the 900 MHZ narrowband TDMA CEPT/GSM mobile radio," in *Proc. IEEE Veh. Technol. Conf.*, San Francisco, CA, Apr. 29–May 3, 1989, pp. 631–639.

[14] A. J. Giger and W. T. Barnett, "Effects of multipath propagation on digital radio," *IEEE Trans. Commun.*, vol. COM-29, pp. 1345–1352, Sept. 1981.

[15] G. Pirani and V. Zingarelli, "Adaptive multiplication-free transversal

equalizers with application to digital radio systems," *IEEE Trans. Commun.*, vol. COM-32, pp. 1025-1033, Sept. 1984.
[16] V. Zingarelli, "Adaptive multiplication-free transversal equalizers for 16-QAM digital radio systems," in *Proc. IEEE Global Telecomm. Conf.*, Atlanta, GA, Nov. 26-29, 1984, pp. 1563-1568.
[17] S. T. Alexander, "A derivation of the complex fast Kalman algorithm," *IEEE Trans. Acoust., Speech, Signal Processing*, vol. ASSP-32, pp. 1230-1232, Dec. 1984.
[18] R. D. Gitlin and F. R. Magee, "Self-orthogonalizing adaptive equalization algorithms," *IEEE Trans. Commun.*, vol. COM-25, pp. 666-672, July 1977.
[19] B. Widrow and E. Walach, "On the statistical efficiency of the LMS algorithm with nonstationary inputs," *IEEE Trans. Inform. Theory*, vol. IT-30, pp. 211-221, Mar. 1984.
[20] S. Haykin, *Introduction to Adaptive Filters*. New York: MacMillan, 1984.
[21] L. Ljung, "Error propagation in adaptation algorithms with poorly exciting signals," *Ann. Télécommun.*, vol. 41, no. 5-6, pp. 322-327, 1986.
[22] L. Ling, D. Manolakis, and J. G. Proakis, "Finite word-length effects in recursive least squares algorithms with application to adaptive equalization," *Ann. Télécommun.*, vol. 41, no. 5-6, pp. 328-336, 1986.
[23] J. M. Cioffi and T. Kailath, "Fast, recursive-least-squares transversal filters for adaptive filtering," *IEEE Trans. Acoust., Speech, Signal Processing*, vol. ASSP-32, pp. 304-337, Apr. 1984.
[24] European Telecommunications Standards Institute (ETSI), Rec. ETSI/GSM 05.04, 1990.
[25] G. D'Aria and V. Zingarelli, "Results on Fast-Kalman and Viterbi adaptive equalizers for mobile radio with CEPT/GSM system characteristics," in *Proc. IEEE Global Telecommunications Conf. (GLOBECOM'88)*, Hollywood, FL, Nov. 28-Dec. 1, 1988, pp. 26.3.1-26.3.5.
[26] J. G. Proakis and F. Ling, "Recursive least squares algorithms for adaptive equalization of time-variant multipath channels," in *Proc. IEEE Int. Conf. on Communications*, Amsterdam, The Netherlands, May 1984, pp. 1250-1254.
[27] J. M. Cioffi, "Block-processing FTF adaptive algorithm," *IEEE Trans. Acoust., Speech, Signal Processing*, vol. ASSP-34, pp. 77-90, Feb. 1986.
[28] E. Eleftheriou and D. D. Falconer, "Adaptive equalization techniques for HF channels," *IEEE J. Select. Areas Commun.*, vol. SAC-5, pp. 238-247, Feb. 1987.
[29] European Telecommunications Standards Institute (ETSI), Rec. ETSI/GSM 05.05, 1990.
[30] K. H. Mueller and D. A. Spaulding, "Cyclic equalization—A new rapidly converging equalization technique for synchronous data communication," *Bell Syst. Tech. J.*, vol. 54, no. 7, pp. 369-406, Feb. 1975.

Giovanna D'Aria was born in Matera, Italy, on May 20, 1959. She received the Dr. Ing. degree in electronic engineering from the Polytechnic of Torino, Torino, Italy, in 1984.

Since 1984 she has been working as Research Engineer in the Radio Transmission Division of CSELT (Centro Studi e Laboratori Telecomunicazioni), Torino. Her main interests include fast adaptive equalization, modulation and coding, performance evaluation, and digital simulation techniques, for both fixed and mobile digital radio systems.

Roberto Piermarini (M'89) was born in Italy on July 25, 1956. He received the Dr. Ing. degree in electrical engineering from the University of L'Aquila, Italy, in 1982.

In 1984 he joined Selenia S.p.A., Rome, Italy, where he was engaged in digital control systems and in switched power supplies for military equipments. Since 1985 he has been with SSGRR (Scuola Superiore Guglielmo Reiss Romoli), the postgraduate school in telecommunications of the STET holding group in L'Aquila, where he is currently in charge of the professional up-dating program in digital communications. His current research interests include digital communications, adaptive filtering and signal processing.

Dr. Piermarini is a member of EURASIP (European Association for Signal Processing) and of the Italian Association of Electrical and Electronic Engineers (AEI).

Valerio Zingarelli (M'82) was born in Italy on May 29, 1953. He received the Dr. Ing. degree in electronic engineering from the Polytechnic of Torino, Torino, Italy, in 1978.

After graduation he gave lectures at the Department of Electronics and Telecommunications of the Polytechnic of Torino. In 1980 he joined CSELT (Centro Studi e Laboratori Telecommunicazioni), the research center of the STET holding group in Torino, where, as a scientist of the Scientific Department, he was engaged in researches on digital communication theory and coding, secure communications and spread spectrum systems, numerical analysis and optimization techniques. Then, with the Radio Transmission Division of CSELT, he was involved in the study of the Italian digital satellite system ITALSAT, of the Pan-European ETSI/GSM digital mobile radio system, and of the European (ETSI) terrestrial microwave radio-relay links. For such systems he performed studies on fast adaptive equalizers, digital modulation and coding techniques, cellular coverage, outage probability computation, and antenna diversity reception techniques. Since 1990 he has been with Alenia (Aeritalia & Selenia), Defence Systems, Torino, in charge of the radio communications research activities in the Direction of Research and Technology Innovation. He is the author of over 30 papers on the above topics and holds two patents on adaptive equalizers and one on dichroic surfaces for electromagnetic systems. His international activities (as a member of the Italian delegations) include CCIR, ETSI, COST, EUROCAE, EAEC, and RTCA.

Dr. Zingarelli is a member of the Italian Association of Electrical and Electronic Engineers (AEI).